

This is the accepted manuscript made available via CHORUS. The article has been published as:

## Hydrodynamic disassembly and expansion of electron-beam-heated warm dense copper

J. E. Coleman, H. E. Morris, M. S. Jakulewicz, H. L. Andrews, and M. E. Briggs

Phys. Rev. E **98**, 043201 — Published 8 October 2018

DOI: [10.1103/PhysRevE.98.043201](https://doi.org/10.1103/PhysRevE.98.043201)

# Hydrodynamic disassembly and expansion of electron beam heated warm dense copper

J.E. Coleman, H.E. Morris, M.S. Jakulewicz, H.L. Andrews, and M.E. Briggs  
*Los Alamos National Laboratory, Los Alamos, NM 87545, USA.*  
(Dated: September 7, 2018)

Cu foils, 200  $\mu\text{m}$  in thickness, were heated in two stages by a  $\sim 100$ -ns-long mono-energetic electron bunch at 19.8 MeV and a current of 1.7 kA ( $8.5 \times 10^{14}$  e-) in a 2-mm-spot to  $T_e \sim 1$  eV. After 45 ns of isochoric heating the pressure in the foil builds upto  $> 20$  GPa (200 kbar), it begins to hydrodynamically disassemble, and a velocity spread is measured. Near the end of the electron pulse the 1550 nm probe is cutoff or absorbed. Photonic doppler velocimetry measurements were made to quantify the expansion velocity, hydrodynamic disassembly time, and pressure of the foil prior to cutoff. Measurements indicate foil motion begins the instant electrons pass through the foil and continues until the particle velocity approaches the ambient sound velocity of Cu and the bulk density exceeds the critical density of the probe. Once the density of the plasma drops below the critical threshold and begins reflecting again, an expansion velocity of the classical plasma is also measured, similar to the point-source solution.

PACS numbers:

## I. INTRODUCTION

Pressure and velocity are essential measurements for the equation-of-state (EOS) in the warm dense matter (WDM) regime. WDM is a low temperature plasma at nearly solid density covering the parameter space of:  $0.1 < T_e$  (eV)  $< 10$  and  $10^{22} < n_e$  ( $\text{cm}^{-3}$ )  $< 10^{24}$  for most metals. WDM is typically strongly coupled ( $\Gamma \sim 1$ ) and degenerate due to the Fermi Energy  $> 1$  eV compared to lower density classical plasmas [1–3]. The EOS and shock Hugoniot for Cu has been investigated in detail for the last 30 years by refs[4–9], however these measurements were done through gas gun shock compression techniques and at this time no plasma properties were measured.

In the plasma physics and shock physics communities velocity measurements are typically made on shock compressed materials and gases over a wide range of pressures. These pressures range from MPa for plate impact experiments on noble gases [10] to TPa for shock compression of MgO [11]. These velocities are typically measured with two techniques: velocity interferometer system for any reflector (VISAR) [12, 13] and photonic Doppler velocimetry (PDV) [14].

VISAR measurements have traditionally been fielded on laser shock compression experiments to measure shock velocity ( $u_s$ ) vs. particle velocity ( $u_p$ ) along the shock Hugoniot. 85 eV blackbody radiation was used to shock compress Be to 360 GPa [15]. 250-300 J of green laser light was used to provide spherical and planar shocks to 0.3-1 mm-thick Si and recorded velocities up to 0.8 km/s [16]. 500 J of laser energy was used to dynamically compress 20-50  $\mu\text{m}$  of MgO and evaluate two crossover points in the Hugoniot at 350 and 650 GPa ( $u_s \sim 15$  and 18 km/s) [11].

PDV has been used to measure initial shocks and flyer plates in gas gun experiments [10, 14, 17]. Ref. [10] measured shocked Ar from plate impact at pressures of 1.4-6.9 MPa. Ref. [14] evaluated initial shock arrival in

explosively driven metal. Ref. [17] measured  $\sim 1$  km/s velocities on the surface of 1-mm-thick ferrite impacted by a 250  $\mu\text{m}$  Mylar flyer. PDV has also been used to measure shock velocities of 250-nm-thick Ti from laser ablated Si [18] and the polymorphic transition of shock compressed Sn up to 44 GPa [19].

As mentioned in a previous review [20], WDM has been produced and characterized by several approaches, the largest contribution is from the laser community. Several authors, only a small subset is referenced here, have produced isochoric heating with sub-ps pulses at peak amplitudes in 0.1-100  $\mu\text{m}$  thick targets [21–24]. In most of these experiments there is a laser prepulse (or a slight contrast) which deposits energy in the foil and generates a preplasma. This preplasma sheath accelerates electrons to a range of energies which in turn provide the heating. The lasers range from a low intensity of  $10^{17}$  W/cm<sup>2</sup> [21] producing 20 keV class electrons to  $2 \times 10^{20}$  W/cm<sup>2</sup> [24], which is estimated to produce electrons with a large range of relativistic energies. These approaches rely heavily on 2D particle-in-cell simulations and collisional Monte Carlo codes to predict both the electron energy distribution and the energy deposition into the target. A stacked Bremsstrahlung spectrometer in combination with Monte Carlo simulations estimated the electron energy distribution ranging from  $10^{14}$  electrons at the low energy end of 1 MeV dropping exponentially below  $10^{11}$  electrons at 14 MeV from laser impact on 600- $\mu\text{m}$ -thick Al-Cu sandwiched targets at an intensity of  $8 \times 10^{19}$  W/cm<sup>2</sup> [23]. Similar estimates were made by ref.[24] indicating just under  $10^{12}$  electrons with energy  $> 4$  MeV dropping exponentially to  $10^7$  electrons at energies of 100 MeV for laser intensities of  $2 \times 10^{20}$  W/cm<sup>2</sup>. Although these experiments claim an isochoric heating process, simulations by ref.[24] indicate the prepulse causes premature energy deposition by lower energy electrons and expansion before the peak of the pulse.

WDM produced directly by particle beam impact has

been investigated with ions through several approaches, but only recently with monochromatic relativistic electrons [20, 25]. GSI has used GeV-class Uranium ions to heat W, Au, and Pb [26, 27]. The NDCX-I and NDCX-II facilities have heated Au and Sn targets [28–32]. Lasers have been used to accelerate protons and  $\text{Al}^+$  ions to heat C and Au samples [34–36]. Ref. [35] measured expansion speeds of 6.7 and 7.5  $\mu\text{m/ns}$  (km/s) for C and Au over a 5 ns window heated by laser accelerated  $\sim 140\text{-MeV}$   $\text{Al}^+$  ions. Ref. [26] measured a 2.6 km/s expansion velocity for a Pb foil heated with 83.3 GeV  $\text{U}^{73+}$  ions. In addition the Pb target pressure and displacement were indirectly measured  $\sim 1 \mu\text{s}$  after heating by measuring the displacement history on volume constraining sapphire plates [37]. These particle beam driven approaches [20, 25, 26, 35] have measured the expansion of the subsequent plasma with optical imaging techniques, but not the target itself. To date there has been no direct measurement of the target dynamics for particle beam driven, collisional, isochoric heating of a solid target: hydrodynamic disassembly time, pressure, and target velocity.

Recently we have begun investigating two-stage heating with a monochromatic 20 MeV, 1.7 kA bunch of electrons [20, 25]. The physics of experiments producing relativistic electron plasmas are much different than direct heating with monochromatic relativistic electrons for several reasons: how the energy is initially deposited, the number of particles providing the heating, heating time scales, and the energy distribution of the particles. We have demonstrated production of a large homogeneous volume ( $3 \times 10^{-4} \text{ cm}^3$ ) and mass (2.8 mg) of warm dense Ti and Cu and measured  $T_e > 1.25 \text{ eV}$  and  $n_e = 3 \times 10^{17} \text{ cm}^{-3}$  in the expanded less degenerate state. In order to help confirm this slower heating technique, relative to isochoric heating techniques performed with short pulse lasers and laser shock-compression experiments, we have fielded a single collimated PDV probe to provide our first EOS measurement. This provides a measurement of the foil velocity, hydrodynamic disassembly time, hydroexpansion of the warm dense copper (WDCu) and get a possible estimate of the lifetime of the warm dense phase. This is the first quantitative set of experiments documenting these parameters.

## II. ISOCHORIC HEATING & HYDRODYNAMIC DISASSEMBLY

In previous reviews the heating and expansion process for electron beam driven Ti & Cu was explained [20, 25]. Briefly, we are performing an identical two-stage heating technique. The first stage, which is considered isochoric, is early in the electron pulse  $t < t_{\text{hydro}}$ .  $t_{\text{hydro}} = \Delta z / 2C_o$  is the hydrodynamic disassembly time of a thin foil, where  $C_o$  is the shock velocity at infinitesimally small particle velocity or the sound velocity at ambient pressure and  $\Delta z$  is the foil thickness.  $C_o$  is 3.93 km/s ( $\mu\text{m/ns}$ ) for Cu, so  $t_{\text{hydro}}$  for a 200- $\mu\text{m}$ -thick Cu foil is

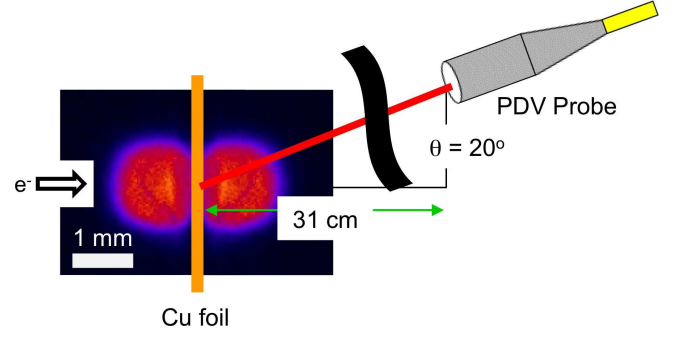


FIG. 1: Experimental setup displaying an electron beam heated Cu foil (not to scale), an expanding plume (false color), and a PDV probe oriented  $20^\circ$  off normal of the foil face on the downstream side. The expanded plume, shown for reference, is the visible light emitted from the plasma over 90 ns, 20 ns after beam energy deposition begins. Scales are shown for reference.

25.4 ns. From the measurements below it is estimated that the isochoric heating process lasts until 45 ns for 200- $\mu\text{m}$ -thick Cu. Prior to this time  $>50\%$  of the  $\rho_o$  remains constant. Simulations indicate a similar performance as will be explained below.

Recent PDV measurements help validate the previously observed adiabatic expansion images and analytic calculations [20, 25]. In addition we are actively measuring the expansion velocity, foil displacement, and pressure in the foils before disassembly. The foils are securely fastened into a rigid target paddle assembly, which can be translated vertically, and provides optical access both upstream and downstream of the foil. A single collimated PDV probe with a working distance of 14 in ( $> 30 \text{ cm}$ ) was installed on a re-entrant tube on the vacuum section (Fig. 1) to bring the probe spot within 500  $\mu\text{m}$  at this working distance. Recall the electron beam spot is 2 mm. The probe was oriented at  $20^\circ$  relative to the foil surface to avoid interference with the electrons transmitted through the foil. The probe orientation is shown with a 90-ns time gated image of the visible light emission from a Cu plume for illustration. Since the probe is at  $20^\circ$  it is measuring  $v_z \cos(20^\circ)$  because the surface has a roughness  $\sim 2 \mu\text{m}$ . Due to the probe wavelength  $\gg$  than the surface roughness of Cu, we are able to measure non-specular backscattering from the rough surface unambiguously [38, 39]. The probe provides a measurement over a large range of velocities with ns temporal resolution and 10  $\mu\text{s}$  of time history. However, this measurement is only done along the probe axis and therefore does not completely capture the spherical plume expansion measured through imaging in [20, 25]. The measurement is very sensitive to alignment and often requires a pilot shot on the foil for precise alignment to within 250  $\mu\text{m}$  of the center of the electron beam spot.

Fig. 2(a) provides an example shot in which we measure the voltage response or beat wave from the PDV

probe of an electron-heated 200- $\mu\text{m}$ -thick Cu foil. Fig. 2(a) shows a 150 ns snap shot while the electron beam is depositing energy compared to the 10- $\mu\text{s}$  window shown in the inset. At  $t = 0$  ns we measure a rapid rise in the signal to 250 mV for close to 5 ns. This is the initial elastic motion of the foil due to electrons hitting the surface, depositing energy, and beginning the melt process, which requires 0.13 J. The electrons are depositing energy at a rate of  $< 0.2$  J/ns. After this point,  $t > 10$  ns, the signal amplitude is reduced by 50%, has a +50 mV bias offset, and the beat wave begins to dampen out from  $\pm 100$  mV at 10 ns to  $\pm 50$  mV for  $t > 25$  ns. The noise level of this signal is  $\sim 25$  mV so the S/N is close to 10 and begins to decrease once the foil disassembles.

Examining the corresponding spectrogram in Fig. 2(b) we see there is a strong velocity band from 0-25 ns with a slope (acceleration)  $\sim 35$  mm/ $(\mu\text{s})^2$ . The velocity spectrogram is calculated from the beat frequency,  $f_{\text{beat}}$ :  $v(t) = cf_{\text{beat}}/2f_o = 1/2f_{\text{beat}}\lambda_o$ , where  $c$  is the speed of light, and  $f_o$  and  $\lambda_o$  are the probe reference frequency and wavelength, 1550 nm. The beat frequency is calculated from the Doppler shifted frequency  $f_D$  measured with respect to the reference probe where  $f_{\text{beat}} = f_D - f_o$ .

Once the  $\langle v \rangle$  in the spectrogram reaches 1.6 mm/ $\mu\text{s}$  (km/s) ( $t = 45$  ns in Figs. 2(b) & 4(a)), the slope in the velocity is reduced, the signal is reduced to  $< 20$  dB, and a  $\sim 15\%$  velocity spread is measured for close to 80 ns. This is an indication of hydrodynamic disassembly of the foil. Ref.[7] indicates plastic deformation of Cu begins at particle velocities,  $u_p$ ,  $> 0.75$  km/s (mm/ $\mu\text{s}$ ) and refs. [8, 17] indicate the measurement of a slow elastic precursor wave prior to the shock breakout (or the plastic wave). It is our belief that we are observing an elastic wave from 0-10 ns, after which the foil begins to accelerate at a fairly constant rate up to 45 ns. Then the material begins to disassemble, a plume forms, and a  $\sim 15\%$  velocity spread is measured. A velocity spread is being measured because the probe is penetrating a Cu plume and a range of fast and slow particles (ejecta, lower density plasma) are crossing the probe path from 45-125 ns. The minimum estimated particle size we can measure is  $> \lambda_o/2$  based on Mie scattering theory [40, 41]. Based on these measurements and observations from hydro simulations below, once the foil begins to disassemble we are transitioning into WDM. This is the first time the temporal evolution of this process has been documented through measurements and hydro simulations; presenting a possible advantage of this slower heating technique.

To help better understand the dynamics of this heating process and compare the measurements to the tabulated EOS, the LASNEX[42] 2D Lagrangian radiation-hydrodynamics code was used to model the expansion of the electron beam heated Cu. These simulations were performed using an axisymmetric geometry and solve the Navier-Stokes equations with artificial viscosity and electron thermal conduction, plus multigroup radiation diffusion. The energy was deposited using a particle beam source; electron beam collisional stopping power and ion-

ization cross sections were used to accurately represent the collisional heating process. Since Cu was the target material used, we used the EOS table SESAME 3336 [9, 43]. The LASNEX model was used to estimate the electron temperature, density, average ionization, motion of the foil surface and pressure within the foil. From these simulations we were able to make a direct comparison of the foil motion and pressure to the PDV measurements. In order to accurately model the experiment, the proper current pulse, energy deposition rate and energy density distribution must be used. 2-dimensional edge effects are not observed for this material, but are easily resolved with axial zone sizes  $< 1$   $\mu\text{m}$  at  $t=0$  and adapting in size to 1.1  $\mu\text{m}$  at 32 ns when the calculated pressure begins to release as indicated below.

The time resolved electron temperature, density, and average ionization at 50 ns intervals are shown in Fig. 3. These are calculated along the axis within the first radial zone which is 17  $\mu\text{m}$ . The initial solid density of Cu is  $7.8 \times 10^{22}$   $\text{cm}^{-3}$  so the peak  $n_e$  increases  $> 3 \times$  in 50 ns due to the higher ionization states during the isochoric heating process (Fig. 3(a)). The pressure builds up in the material during the heating process and then it releases, WDCu forms, and expansion begins. The electron density decreases to  $1.3n_o$  at 100 ns and continues to drop as the material expands but remains in the warm dense phase for  $> 200$  ns. The electron density does not drop below the cutoff density for the PDV probe until we are 500- $\mu\text{m}$  from the target center at 150 ns.

In the first 50 ns, while the heating is isochoric, the calculated temperature ranges from 0.5 eV at the edge to 0.65 eV near the center (Fig. 3(b)). After this point, WDCu exists and we continue to dump energy into the expanding plasma, heating it to just under 0.95 eV at the center at 100 ns. Later in time the calculated  $T_e$  drops back to 0.6 eV 500- $\mu\text{m}$  from the center at 150 ns and  $> 0.5$  eV 600- $\mu\text{m}$  from target center at 200 ns. Heating to these temperatures  $\text{Cu}^{3+}$  ions may exist near the target center and begin to relax to average ionization levels above  $\text{Cu}^+$  for  $> 200$  ns (Fig. 3(c)). These ionization states at 150 and 200 ns agree well with spectroscopy measurements made during this time frame with a thinner foil in [25].

We have examined the initial hydroexpansion of the 200- $\mu\text{m}$ -thick foils for 3 consecutive shots during this heating process and see  $< 10\%$  variation in the leading edge velocity. The leading edge velocity is defined as the maximum measured velocity in the spectrogram where the minimum signal is  $12 \pm 2$  dB. For illustration we only show the results from shot 25901 in comparison with the LASNEX simulation in Fig. 4. First we examine the mean velocity from the spectrogram in Fig. 2(b) and we compare it to the leading edge to get the maximum particle motion (Fig. 4(a)). The average velocity profile is calculated by selecting a region-of-interest from the spectrogram in Fig. 2(b) within a signal threshold of 10 dB. The mean velocity indicates a linear ramp instantly and increases to  $\langle v \rangle = 1.6$  mm/ $\mu\text{s}$  at 45 ns, where it begins to flatten out. Examining the fastest particle

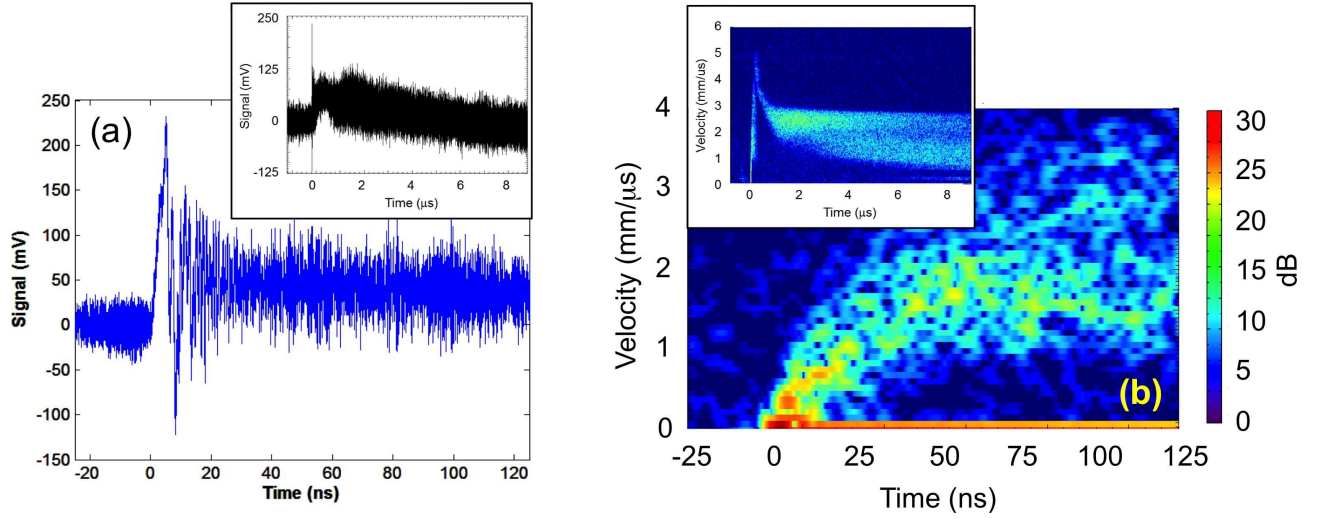


FIG. 2: (a) Zoomed in version of the measured voltage response on the PDV probe with electrons incident on the foil at  $t = 0$ ; the full 10- $\mu$ s record is shown on the inset; (b) the calculated velocity spectrogram for this 150 ns window is shown indicating the hydro-motion of the foil; the full 10- $\mu$ s spectrogram is shown on the inset. All data for shot number 25901.

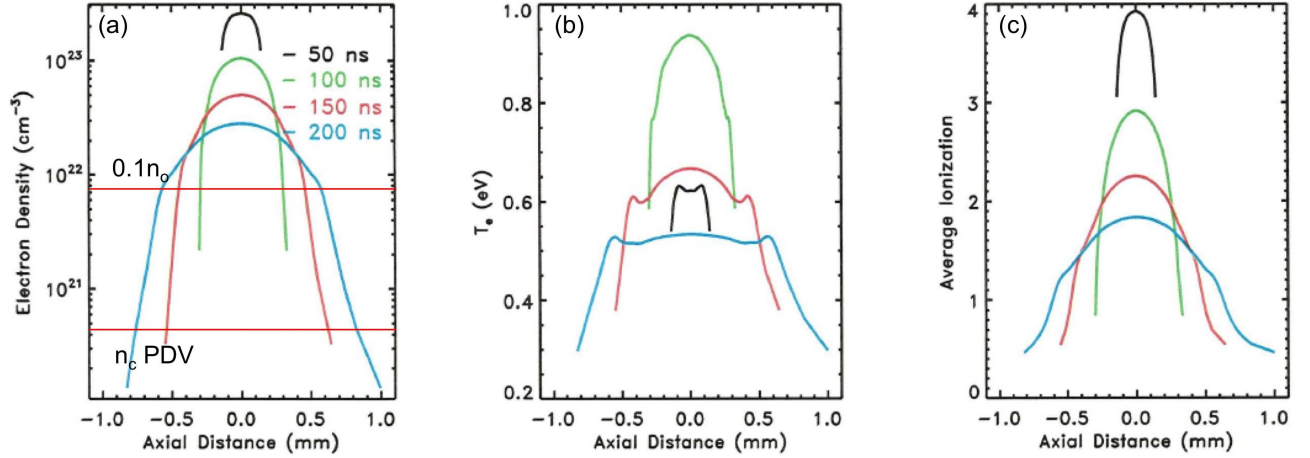


FIG. 3: LASNEX calculation of the axial electron (a) density; (b) temperature and; (c) ionization state for an 200- $\mu$ m Cu foil at 50 ns intervals from 50-200 ns. 10% solid density is indicated in addition to the critical density for PDV in Fig. 3(a).

movement from the leading edge of the spectrogram we see a faster acceleration  $\sim 50 \text{ mm}/(\mu\text{s})^2$  for the first 50-60 ns. The acceleration of the leading edge also slows down, just after 100 ns we measure peak velocities near  $4 \text{ mm}/\mu\text{s}$ . The calculated velocity from LASNEX has a similar velocity slope with the leading edge until  $\sim 70$  ns, after which the slope is reduced but extends above the measurement. Keep in mind this calculation neglects the cutoff density effect, which limits the experimental probe in measuring the peak velocity after warm dense matter is formed.

By simply integrating the measured velocity  $v$  we can calculate the foil displacement at the edge,  $\delta z = z_0 + \int v(t)dt$ . The average expanded location of the foil face is indicated in Fig. 4(b). The initial movement is slow,

then the expansion rate tends to increase at a steady rate, the average expansion is  $< 200 \mu\text{m}$ . The leading edge indicates a maximum particle displacement  $> 300 \mu\text{m}$  away from the original surface and this tends to agree fairly well with the EOS calculation in LASNEX. Now keep in mind this is the estimated foil movement at the edge from a velocity measurement and is not necessarily representative of movement of the whole foil volume. In addition there may be small errors in the displacement due to the probe being  $20^\circ$  off normal [39]. During the initial expansion, prior to disassembly, we can calculate the pressure in the elastic limit:  $P_E(t) = 1/2 C_o v(t) \rho(t)$ , where  $\rho(t)$  is the calculated density derived from the measured expanded volume  $V(t) = V_0 + 2A\delta z$  and the heated mass of material interrogated by the probe. This is an ap-

proximation because the volume is expanding spherically, but the probe can only measure the expansion along the probe axis [38, 39].  $A$  is the initial heated area of the foil. As stated above once the average velocity reaches  $1.6 \pm 0.2$  mm/ $\mu$ s, nearly 45 ns after energy deposition begins (Fig. 2(b) & 4(a)), the average pressure exceeds 20 GPa (200 kbar) and then the material begins to release or hydrodynamically disassemble (Fig. 4(c)). We see a similar trend with the leading edge, reduced acceleration tends to coincide with a pressure release at a slightly later time compared to the average case; the peak pressure we infer from measurements is near 25 GPa. We calculate a slightly faster rise in pressure with LASNEX and a peak pressure of 32 GPa, 20% higher than the experiment. This pressure is calculated at the center 800 nm axial zone and the center 17  $\mu$ m radial zone of the foil; the calculated pressure averaged along the entire axis at disassembly is 24 GPa. Each of these is fairly close to the solid-density Fermi pressure of 33 GPa [44]. In addition this pressure is close to the tabulated shock Hugoniot data at 5 km/s [45], which is the maximum velocity we measure at 160 ns (Fig. 5). The electrons are uniformly heating the foil through collisions with Cu atoms, stripping electrons from the atom, increasing temperature and pressure throughout the volume. This is isochoric heating until the material disassembles and releases pressure, since  $>50\%$  of  $\rho_o$  remains constant until this point. We do not believe there is a shock based on these observations and the agreement with the EOS table SESAME 3336 [9, 43]. Pressure evaluation with the Hugoniot relations is at least  $3\times$  higher.

Despite the foil beginning to hydrodynamically disassemble at 45 ns, which is also where we begin to generate WDM, we still continue to measure particle velocities well beyond the 100 ns pulse length of the electron beam (Fig. 5). We measure a velocity range of 1-4 mm/ $\mu$ s over 45-250 ns time window. We reach a peak velocity of 4 mm/ $\mu$ s near 120 ns and above this point the signal is cutoff and there are no longer any particles in the probe path with a velocity greater than this until 160 ns. The cutoff density for 1550 nm is  $4.6 \times 10^{20}$  cm $^{-3}$  which is  $\sim 200\times$  below solid density Cu ( $7.8 \times 10^{22}$  cm $^{-3}$ ). We believe during this 120-160 ns time window the probe is being absorbed or strongly attenuated by the dense material it is path, then it proceeds to expand and cool off. Higher velocities may exist, as calculated by LASNEX, at  $t < 160$  ns from the higher temperature, dense plasma but they are not measured due to absorption of the 1550 nm light. Near 160 ns we measure a peak velocity of 5 mm/ $\mu$ s and beyond that point we measure the expansion of the recombining classical plasma.

### III. ADIABATIC EXPANSION

As indicated from the LASNEX calculations (Fig. 3) and measurements in Fig. 5, 120 ns after disassembly begins ( $t = 160$  ns), the density, 400- $\mu$ m from the origi-

nal foil edge, drops below the cutoff and the plasma begins cooling; at this point we begin measuring the slowing down velocity of the adiabatically expanding plasma. The initial velocity band we measure at 160 ns is 4.4-5.0 mm/ $\mu$ s. Examining Figs. 2(b) & 5 more closely we can see the particle velocity reduces down to a range of 1.9-3.0 mm/ $\mu$ s at 1  $\mu$ s and continues to slow down to 0.9-2.8 mm/ $\mu$ s at 5  $\mu$ s and 0.57-2.7 mm/ $\mu$ s at 9  $\mu$ s. Although we see a significant slowing down feature we also have particles maintaining  $v > 2.7$  mm/ $\mu$ s for close to 10  $\mu$ s. Clearly indicating we have a range of velocities due to a plume expanding close to  $\sim 1$  cm along the direction of the probe path. Performing a fit to the slowest velocities over the 1-7  $\mu$ s band in Fig. 2(b) we obtain  $v(t) \sim t^{-0.76}$ , which is a slightly slower deceleration than we observed from images in ref. [25] and expected from the point-source solution [46-48].

### IV. CONCLUSION

We have fielded the first PDV probe and demonstrated time-resolved velocity measurements on a Cu foil heated purely by electrons in a two-stage process. The voltage response on the PDV probe indicates a short  $\sim 10$  ns elastic precursor and a  $t_{hydro} = 45$  ns for an 200- $\mu$ m-thick foil. These measurements indicate the release at  $\langle v \rangle$  and  $\langle P \rangle$  of 1.6 mm/ $\mu$ s (km/s) and 21 GPa. The pressure is calculated assuming an elastic expansion since we are isochorically heating during this first stage and there is no presence of a shock. The measured peak pressure agrees reasonably well with LASNEX simulations and the calculated Fermi pressure. After the material releases and WDM is formed a range of velocities is measured due to the probe being intersected by an expanding plume.

A peak expansion velocity of 4 mm/ $\mu$ s (km/s) is measured prior to the probe being cutoff or absorbed. The velocity distributions are extremely repeatable with identical foils and precise alignment of the probe. There are visible trends of reduced  $t_{hydro}$ , foil deflection, and pressure for thinner foils, but the relationship is not linear. We also measure a slow-down velocity spectrum which agrees fairly well with the observed adiabatic expansion from previous plume images and analytic approximations. These measurements are the first of their kind, confirming the onset of hydrodynamic disassembly for an electron beam heated foil, the generation of a warm dense plasma, and the existence of WDM  $> 200$  ns.

### Acknowledgments

This work was supported by the National Nuclear Security Administration of the U.S. Department of Energy under Contract No. DE-AC52-06NA25396. We would like to thank C.A. Bolme, W.T. Buttler, J. Danielson, C.A. Ekdahl, J.P. Harding, R. Hixson, S.D. McGrane, and G. Rodriguez for their technical discussions. We



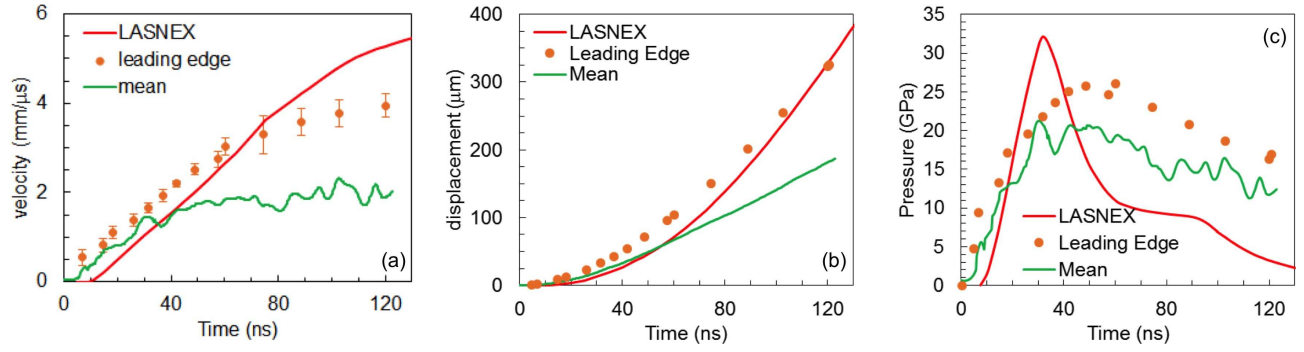


FIG. 4: Red: LASNEX calculation of the maximum particle velocity, Orange dots: experimentally measured values from the leading edge of the spectrogram in Fig. 2(b), Green: mean of the experimentally measured spectrogram. (a) particle velocity; (b) foil displacement at the edge and; (c) elastic pressure, from a 200- $\mu\text{m}$ -thick copper foil for shot number 25901.

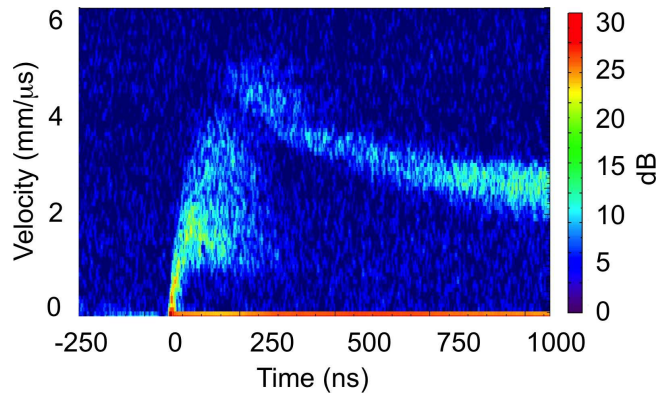


FIG. 5: An expanded velocity spectrogram out to 1  $\mu\text{s}$  from the same foil hydro-motion from Fig. 2(b) indicating the temporal velocity spread and cutoff time for shot number 25901.

would like to take the opportunity to thank Don Roeder and Sharon Dominguez for their manufacturing and design support. We would like to thank the operators, technicians, and engineers Doug Aikin, Robbie Brooks, Jules Carson, Josh Esquibel, Raul Gonzalez, Kris Peterson, Melissa Reed, Tony Sanchez, Sam Snider, Rudy Valdez, and Travis Weaver for their continued support.

- 
- [1] Committee on High Energy Density Plasma Physics, National Research Council, *Frontiers in High Energy Density Physics: The X-Games of Contemporary Science*, The National Academies Press, Washington, DC, (2003).
  - [2] R.W. Lee, S.J. Moon, H.K. Chung, W. Rozmus, H.A. Baldis, G. Gregori, R.C. Cauble, O.L. Landen, J.S. Wark, A. Ng, S.J. Rose, *J. Opt. Soc. Am. B* **20**, 770 (2003).
  - [3] A.B. Zylstra, J.A. Frenje, P.E. Grabowski, C.K. Li, G.W. Collins, P. Fitzsimmons, S. Glenzer, F. Graziani, S.B. Hansen, S.X. Hu, M. Gatu Johnson, P. Keiter, H. Reynolds, J.R. Rygg, F.H. Sguin, and R. D. Petrasso, *Phys. Rev. Lett.*, **114**, 215002 (2015).
  - [4] A.C. Mitchell and W.J. Nellis, *J. Appl. Phys.* **52**, 3363 (1981).
  - [5] A.C. Mitchell, W.J. Nellis, J.A. Moriarty, R.A. Heinle, N.C. Holmes, R.E. Tipton, and G.W. Repp, *J. Appl. Phys.* **69**, 2981 (1991).
  - [6] W.J. Nellis, A.C. Mitchell, and D.A. Young, *J. Appl. Phys.* **93**, 304 (2003).
  - [7] E.M. Bringa, J.U. Cazamias, P. Erhart, J. Stölken, N. Tanushev, B.D. Wirth, R.E. Rudd, and M.J. Caturla, *J. Appl. Phys.* **96**, 3793 (2004).
  - [8] R. Chau, J. Stölken, P. Asoka-Kumar, M. Kumar, and N. C. Holmes, *J. Appl. Phys.* **107**, 023506 (2010).
  - [9] J.H. Peterson, K.G. Honnell, C. Greeff, J.D. Johnson, J. Boettger, and S. Crockett, *AIP Conference Proceedings* **1426**, 763 (2012).
  - [10] D.M. Dattelbaum, P.M. Goodwin, D.B. Garcia, R.L. Gustavsen, J.M. Lang, T.D. Aslam, S.A. Sheffield, L.L. Gibson, and J.S. Morris, *AIP Conference Proceedings* **1793**, 090004 (2017).
  - [11] K. Miyanishi, Y. Tange, N. Ozaki, T. Kimura, T. Sano, Y. Sakawa, T. Tsuchiya, and R. Kodama, *Phys. Rev. E* **92**, 023103 (2015).
  - [12] L.M. Barker and R.E. Hollenbach, *J. Appl. Phys.* **43**, 4669 (1972).
  - [13] P.M. Celliers, D.K. Bradley, G.W. Collins, D.G. Hicks, T.R. Boehly, and W.J. Armstrong, *Rev. Sci. Instrum.* **75**, 4916 (2004).
  - [14] O.T. Strand, D.R. Goosman, C. Martinez, T.L. Whitworth, and W.W. Kuhlow, *Rev. Sci. Instrum.* **77**, 083108 (2006).

- [15] P.M. Celliers, D.J. Erskine, C.M. Sorce, D.G. Braun, O.L. Landen, and G.W. Collins, *Rev. Sci. Instrum.* **81**, 035101 (2010).
- [16] R.F. Smith, C.A. Bolme, D.J. Erskine, P.M. Celliers, S. Ali, J.H. Eggert, S.L. Brygoo, B.D. Hammel, J. Wang, and G.W. Collins, *J. Appl. Phys.* **114**, 133504 (2013).
- [17] S. Liu, D. Wang, T. Li, G. Chen, Z. Li, and Q. Peng, *Rev. Sci. Instrum.* **82**, 023103 (2011).
- [18] A.R. Valenzuela, G. Rodriguez, S.A. Clarke, and K.A. Thomas, *Rev. Sci. Instrum.* **78**, 013101 (2007).
- [19] C. Chauvin, Z. Bouchkour, F. Sinatti, and J. Petit, *AIP Conference Proceedings* **1793**, 060013 (2017).
- [20] J.E. Coleman and J. Colgan, *Phys. Rev. E* **96**, 013208 (2017).
- [21] K. Eidmann, U. Andiel, F. Pisani, P. Hakel, R.C. Mancini, G.C. Junkel-Vives, J. Abdallah, and K. Witte, *J. Quant. Spectrosc. Radiat. Transfer* **81**, 133 (2003).
- [22] F. Perez, L. Gremillet, M. Koenig, S.D. Baton, P. Audebert, M. Chahid, C. Rousseaux, M. Drouin, E. Lefebvre, T. Vinci, J. Rassuchine, T. Cowan, S.A. Gaillard, K.A. Flippo, and R. Shepherd, *Phys. Rev. Lett.*, **104**, 085001 (2010).
- [23] F. Perez, S.D. Baton, M. Koenig, C.D. Chen, D. Hey, M.H. Key, S. Le Pape, T. Ma, H.S. McLean, A.G. MacPhee, P.K. Patel, Y. Ping, F.N. Beg, D.P. Higginson, C.W. Murphy, H. Sawada, B. Westover, T. Yabuuchi, K.U. Akli, E. Giraldez, M. Hoppe, Jr., C. Shearer, R.B. Stephens, L. Gremillet, E. Lefebvre, R.R. Freeman, G.E. Kemp, A.G. Krygier, L.D. Van Woerkom, R. Fedosejevs, R.H. Friesen, Y.Y. Tsui, and D. Turnbull, *Phys. Plasmas* **17**, 113106 (2010).
- [24] M. Schollmeier, A.B. Sefkow, M. Geissel, A.V. Arefiev, K.A. Flippo, S.A. Gaillard, R.P. Johnson, M.W. Kimmel, D.T. Offermann, P.K. Rambo, J. Schwarz, and T. Shimada, *Phys. Plasmas* **22**, 043116 (2015).
- [25] J.E. Coleman and J. Colgan, *Phys. Plasmas* **24**, 083302 (2017).
- [26] P.A. Ni, F.M. Bieniosek, M. Leitner, B.G. Logan, R.M. More, P.K. Roy, D.H.H. Hoffmann, D. Fernengel, A. Hug, J. Menzel, S. Udre, N.A. Tahir, D. Varentsov, H. Wahl, M. Kulish, D.N. Nikolaev, V.Ya., A. Fertman, A.A. Golubev, B.Yu. Sharkov, and J.J. Barnard, in *Proceedings of the Particle Accelerator Conference*, Albuquerque NM, 2007, p. 2038.
- [27] P.A. Ni, M.I. Kulish, V. Mintsev, D.N. Nikolaev, V.Ya. Ternovoi, D.H.H. Hoffmann, S. Udre, A. Hug, N.A. Tahir, and D. Varentsov, *Laser and Particle Beams* **26**, 583 (2008).
- [28] J.E. Coleman, Ph.D. Thesis, University of California, Berkeley, 2008.
- [29] F.M. Bieniosek, J.J. Barnard, A. Friedman, E. Henestroza, J.Y. Jung, M.A. Leitner, S. Lidia, B.G. Logan, R.M. More, P.A. Ni, P.K. Roy, P.A. Seidl, W.L. Waldron, *Journal of Physics: Conference Series* **244**, 032028 (2010).
- [30] P.A. Ni, F.M. Bieniosek, E. Henestroza, S.M. Lidia, *Nucl. Instrum. Methods Phys. Res., Sect. A* **733**, 12 (2014).
- [31] P.A. Seidl, A. Persaud, W.L. Waldron, J.J. Barnard, R.C. Davidson, A. Friedman, E.P. Gilson, W.G. Greenway, D.P. Grote, I.D. Kaganovich, S.M. Lidia, M. Stettler, J.H. Takakuwa, T. Schenkel, *Nucl. Instrum. Methods Phys. Res., Sect. A* **800**, 98 (2015).
- [32] P.A. Seidl, J.J. Barnard, R.C. Davidson, A. Friedman, E.P. Gilson, D. Grote, Q. Ji, I.D. Kaganovich, A. Persaud, W.L. Waldron, and T. Schenkel, *Journal of Physics: Conference Series* **717**, 012079 (2016).
- [33] P.A. Seidl, private communication.
- [34] A. Pelka, G. Gregori, D.O. Gericke, J. Vorberger, S.H. Glenzer, M.M. Gunther, K. Harres, R. Heathcote, A.L. Kritcher, N.L. Kugland, B. Li, M. Makita, J. Mithen, D. Neely, C. Niemann, A. Otten, D. Riley, G. Schuermann, M. Schollmeier, A. Tauschwitz, and M. Roth, *Phys. Rev. Lett.*, **105**, 265701 (2010).
- [35] W. Bang, B.J. Albright, P.A. Bradley, D.C. Gautier, S. Palaniyappan, E.L. Vold, M.A. Santiago Cordoba, C.E. Hamilton, and J.C. Fernandez, *Sci. Rep.* **5**, 14318 (2015).
- [36] W. Bang, B.J. Albright, P.A. Bradley, E.L. Vold, J.C. Boettger, and J.C. Fernandez, *Phys. Rev. E* **92**, 063101 (2015).
- [37] M. Kulish, A. Fertman, A. Golubev, A. Tauschwitz, and V. Turtikov, *Rev. Sci. Instrum.* **72**, 2294 (2001).
- [38] D.H. Dolan, *AIP Conference Proceedings* **1195**, 589 (2009).
- [39] M.E. Briggs, E.A. Moro, M.A. Shinas, S. McGrane, and D. Knierim, *Journal of Physics: Conference Series* **500**, 142005 (2014).
- [40] S. K. Monfared, W. T. Buttler, D. K. Frayer, M. Grover, B. M. LaLone, G. D. Stevens, J. B. Stone, W. D. Turley, and M. M. Schauer, *J. Appl. Phys.* **117**, 223105 (2015).
- [41] M.M. Schauer, W.T. Buttler, D.K. Frayer, M. Grover, B.M. LaLone, S.K. Monfared, D.S. Sorenson, and G.D. Stevens, *J. dynamic behavior mater.* **3**, 217 (2017).
- [42] G.B. Zimmerman and W.L. Kruer, *Comments Plas. Phys.* **2**, 51 (1975).
- [43] The SESAME EOS library is a binary, tabular compendium of equations of state for numerous materials and is maintained and disseminated by Group T-1 at the Los Alamos National Laboratory (email: sesame@lanl.gov).
- [44] R. Paul Drake, *High-Energy-Density Physics: Foundation of Inertial Fusion and Experimental Astrophysics*, Second Edition, Springer (2017).
- [45] Los Alamos Shock Hugoniot Data, edited by S.P. Marsh (University of California Press, Berkeley, 1979).
- [46] H.A. Bethe, K. Fuchs, J.O. Hirschfelder, J.L. Magee, R.E. Peierls, and J. von Neumann, "BLAST WAVE", Los Alamos Report LA-2000, Ch.2, (1947).
- [47] G.I. Taylor, *Proc. Roy. Soc. A* **201**, 159 (1950).
- [48] G.I. Taylor, *Proc. Roy. Soc. A* **201**, 175 (1950).